Saudi Journal of Biological Sciences 30 (2023) 103752

HOSTED BY

Contents lists available at ScienceDirect

Saudi Journal of Biological Sciences

journal homepage: www.sciencedirect.com

Original article

Hub genes identification and association of key pathways with hypoxia in cancer cells: A bioinformatics analysis

Faiza Aziz, Naila Shoaib, Abdul Rehman *

Institute of Microbiology and Molecular Genetics, University of the Punjab, Quaid-e-Azam Campus, 54590 Lahore, Pakistan

ARTICLE INFO

Article history:
Received 6 July 2023
Revised 17 July 2023
Accepted 22 July 2023
Available online 27 July 2023

Keywords:
Hypoxic environment
Metabolic pathways
Human cell lines
Differentially expressed genes
Targeted therapies

ABSTRACT

Three human cancer cell lines (A549, HCT116, and HeLa) were used to investigate the molecular mechanisms and potential prognostic biomarkers associated with hypoxia. We obtained gene expression data from Gene Expression Omnibus (GEO) datasets GSE11704, GSE147384, and GSE38061, which included 5 hypoxic and 8 control samples. Using the GEO2R tool and Venn diagram software, we identified common differentially expressed genes (cDEGs). The cDEGs were then subjected to Gene ontology (GO) and Kyoto Encyclopedia of Gene and Genome (KEGG) pathway analysis by employing DAVID. The hub genes were identified from critical PPI subnetworks through CytoHuba plugin and these genes' prognostic significance and expression were verified using Kaplan-Meier analysis and Gene Expression Profiling Interactive Analysis (GEPIA), respectively. The research showed 676 common DEGs (cDEGs), with 207 upregulated and 469 downregulated genes. The STRING analysis showed 673 nodes and 1446 edges in the PPI network. We identified 4 significant modules and 19 downregulated hub genes. GO analysis revealed all of them were majorly involved in ribosomal large subunit assembly and biogenesis, rRNA processing, ribosome biogenesis, translation, RNA & protein binding frequently at the sites of nucleolus and nucleoplasm while 11 were significantly associated with a better prognosis of hypoxic tumors. Our research sheds light on the molecular mechanisms that underpin hypoxia in human cancer cell lines and identifies potential prognostic biomarkers for hypoxic tumors.

1. Introduction

Cancer is a devastating public health issue causing significant global challenges (Hiatt and Beyeler, 2020; Leng et al., 2019). With limited treatment options that often yield poor pro[gnosis and high mortality rates, the medical community is constantly striving to develop more effective methods of treatment (Ferrari et al., 2021). The current treatments rely primarily on chemotherapy, radiation therapy, and targeted therapy (Rosenbaum and Gonzalez, 2021). Unfortunately, it has become increasingly difficult to combat cancer as the cancer cells continuously gain resistance to these treatments due to a range of intrinsic and extrinsic factors (Fares et al., 2019; Hu-Lieskovan et al., 2021; Ulldemolins et al., 2021). Extrinsic factors, such as hypoxia, significantly impact the growth and spread of cancer, making it difficult to target effectively and fully eradicate cancer cells (Ponomarev et al., 2022). Hypoxia develops in most solid tumors, which outstrips the capacity of the newly formed vasculature to provide adequate oxygen (Muz et al., 2015). It has a variety of consequences on the biological behavior of cancer cells, including neovascularization, metabolism, cell survival, and cell death. Hypoxia is a prominent pathogenic hallmark of solid tumors (Tan et al., 2021). Furthermore, it has been shown to confer cancer stem-cell-like properties, such as resistance to treatment, which is a major concern in the medical world. The adaptation processes of cancer cells to hypoxic conditions are regulated by the HIF, NFκB, PI3K, and MAPK pathways, which are transcriptional programs activated by hypoxia (Muz et al., 2015) that may aid in the development of targeted therapies for hypoxic tumors.

Hypoxia has long been recognized as contributing to increased tumor progression and aggressiveness, leading to poorer patient prognosis and survival (Dekker et al., 2022). According to studies,

* Corresponding author at: Institute of Microbiology & Molecular Genetics, University of the Punjab, Lahore, Pakistan.
E-mail addresses: faiza2.phd.mmg@pu.edu.pk (F. Aziz), nailashoaib.crc@pu.edu.pk (N. Shoaib), rehman.mmg@pu.edu.pk (A. Rehman).

Peer review under responsibility of King Saud University.

Production and hosting by Elsevier

https://doi.org/10.1016/j.sjbs.2023.103752
1319-562X/

individuals with hypoxic tumors are more susceptible to metastasis and death (Jiang et al., 2021). To ascertain the hypoxic phenomenon and to target it effectively, researchers are now focusing on dissecting the hypoxia-inducible responses and signaling pathways (Baxevanis and Bader, 2020; Lee et al., 2020; Fojtík et al., 2021). Thanks to the technology, these targets can be achieved through the utilization of bioinformatics and data mining, these tools can help to verify various genes that are expressed differently in two different conditions, allowing them to make better comparisons between them (Baxevanis and Bader, 2020). Additionally, gene expression profiling arrays can also be employed to investigate further the various metabolic and signaling pathways of cancer under hypoxic conditions (Bartoszewski et al., 2019). With the advancements in these fields, novel targets have emerged with the potential to combat hypoxia in the near future.

This study sought to understand better and elucidate the fundamental genes and signaling pathways driving cancer progression in hypoxic conditions, aiming to improve cancer prognosis and treatment. An integrative bioinformatics analysis was performed on various cancer cell lines to identify differentially expressed genes (DEGs), analyze their protein–protein interaction networks, significant modules, and hub genes, determine functional annotations, and assess their potential prognostic value. This study also employed the Kaplan-Meier method to analyze the survival rate associated with hub genes to better comprehend the intricate molecular biology behind hypoxic tumors. We hoped to identify new genes and the significant pathways that could serve as diagnostic biomarkers, prognostic indicators, or potential targets for precise treatment. Our research could allow us a deeper comprehension of potential molecular mechanisms as well as the development of preventive and therapeutic strategies. With the help of the findings from this study, future research can be conducted to understand better the hypoxia implications in cancer progression and resistance, as well as to develop a variety of therapeutic modalities that can be tested in pre-clinical and clinical trials.

2. Materials and methods

2.1. Microarray data and GEO database

The Gene Expression Omnibus (GEO) database contains a wealth of data from high-throughput functional genomic studies. These studies involve the processing and normalization of data through various methods. Using the keywords "Homo sapiens" (organism), "Hypoxia" (study keyword), "A549" (cell line), "HCT116" (cell line), "HeLa" (cell line) and "Expression profiling by array" (study type), we searched for publicly available studies in the GEO database (https://www.ncbi.nlm.nih.gov/geo/). This research identified 3 GEO series in which cells were exposed to 1% hypoxia and 21% O_2 (normoxia) for 24 h. The selection criteria for the studies included the following: (1) cancer cell line (A549, HCT116, HeLa) under hypoxic and normoxic conditions, (2) gene expression profiling of mRNA. The expression profiles of GSE11704, GSE147384, and GSE38061 were subsequently retrieved from the GEO database for investigation.

2.2. Differentially expressed genes (DEGs) identification

In the current investigation, DEGs among hypoxic and normoxic conditions were analyzed using GEO2R (https://www.ncbi.nlm.nih.gov/geo/geo2r/) online tool on the NCBI-GEO website, which uses the limma R packages and GEO query for the analysis of high-throughput genomic data with $|\log_2 FC|>2$ and the threshold for differentially expressed genes (DEGs) was set at a p-value of less than 0.05. Hypoxia-effect biomarkers were defined as DEGs with a p-value less than 0.05 and a fold change (|FC|) greater than 0 in all three datasets. Venn diagrams were created using the Venn diagram program (https://bioinformatics.psb.ugent.be/webtools/Venn/) to illustrate the DEG overlap among the three selected datasets.

2.3. Functional analysis of GO and KEGG pathways

The common DEGs (cDEGs) were analyzed for their Gene ontology (GO) enrichment and KEGG pathway analysis, utilizing a web-based application: Database for annotation, visualization, and integrated discovery (DAVID) developed by the Laboratory of Human Retrovirology and Immunoinformatic (ncifcrf.gov). The GO analysis covered biological processes, cellular components, and molecular functions. A *t*-test (ANOVA) was applied as a default statistical analysis with a p-value greater than 0.05. cDEGs were mapped to KEGG pathways as pathway functional analysis with thresholds count >0 and p-value <0.05.

2.4. PPI network construction

The protein–protein interaction network (PPI) was generated using the online database of Search Tool for the Retrieval of Interacting Genes (STRING), version 11.5 (string-db.org). To ensure statistically significant results, PPI networks of upregulated and downregulated DEGs were generated as full string networks in which the edges indicate both physical and functional interactions with the highest confidence score: of 0.900 and hidden the unconnected nodes in the data. The PPI analysis was then imported into Cytoscape (version 3.7.2) in order to visualize the PPI network.

2.5. Hub genes

The core subgroups, in the PPI network, were identified using module analysis, which included genes with the same expression patterns appearing under many circumstances. Relevant modules were extracted from the PPI network using Cytoscape's Molecular Complex Detection (MCODE) plugin, with a degree cut-off of 2, max depth of 100, node score cut-off of 0, and k-core of 2, MCODE score >5, and nodes $\geq$10 thresholds. The PPI network has a number of nodes and edges that, respectively, represent proteins and their interactions. The PPI network was searched for common hub genes (cHubGs) using the Cytoscape cytoHubba plugin. A node is regarded as the highest ranking cHubGs if it has the most significant connections, interactions, or edges with other nodes. The common Hub genes were chosen by analyzing the topological Degree algorithm of the PPI network. These hub genes were subjected to another round of GO analysis, and the functional enrichment of prognostic genes was determined.

2.6. Common hub genes (cHubGs)

To comprehend the potential biological domains and pathways of the 19 selected hub genes, Gene ontology, and KEGG pathway enrichment was re-analyzed via DAVID ($P < 0.05$).

2.7. Hub gene expression and prognostic value

Given the complexity of cancer, its etiopathogenesis is thought to be the result of multiple interactions and compound gene expression. RNA sequencing expression data available on "Gene Expression Profiling Interactive Analysis GEPIA 2 (cancer-pku.cn)" a website tool that can perform principal component analysis (PCA) of genes and present results in 2D plots, were analyzed to investigate the potential clinical importance of hub genes. It uses the information regarding the hub gene's RNA sequencing expression, including

hundreds of samples from the GTEx studies and TCGA. In addition, the Kaplan-Meier analysis was implemented to perform survival analysis on several cancer types, including colon adenocarcinoma (COAD), cervical squamous cell carcinoma and endocervical adenocarcinoma (CESC), and lung adenocarcinoma (LUAD). The hazard ratio (HR), log-rank P value, and 95% confidence intervals were determined using this internet tool and presented in the plot. Furthermore, the comparison of multiple hub genes provided a reference for assessing the prognosis of various genes in different cancer species.

3. Results

3.1. DEGs identification under hypoxic conditions

The gene expression datasets GSE11704, GSE147384, and GSE38061 were analyzed to identify DEGs between hypoxic and normoxic samples in A549, HCT116, and HeLa cell lines. In the current study, 5 hypoxic and 8 control samples were used. The volcano plots were used to display the DEGs in each dataset (Fig. 1a-c). GEO2R online tool identified 8854 DEGs with 4337 upregulated and 4517 downregulated genes in GSE11704; 3501 DEGs with 1762 upregulated and 1739 downregulated genes in GSE147384; and 41,379 DEGs with 36,732 upregulated and 4647 downregulated genes in GSE38061 with |logFC| > 0 (p-value < 0.05). According to Venn diagram software, there were 676 genes differentially expressed as cDEGs in all three datasets, including 207 upregulated DEGs and 469 downregulated DEGs in hypoxic conditions compared to normoxia (Fig. 1d, e; Table S1).

3.2. DEGs GO functions

DAVID software was employed to perform GO and KEGG analyses on the 676 cDEGs to investigate their functional and biological properties. The top five significantly enriched GO terms of hypoxic conditions (Table 1; Fig. S1). Gene ontology research findings showed that 1) for biological processes (BP), the top five upregulated DEGs were significantly enriched in response to hypoxia, cellular response to hypoxia, glycolytic process, canonical glycolysis, positive regulation of the apoptotic process, and downregulated DEGs were enriched in mitochondrial translation, translation, positive regulation of telomerase RNA localization to Cajal body, rRNA processing, protein folding, 2) In terms of cell components (CC), upregulated cDEGs were significantly enriched in the cytosol,

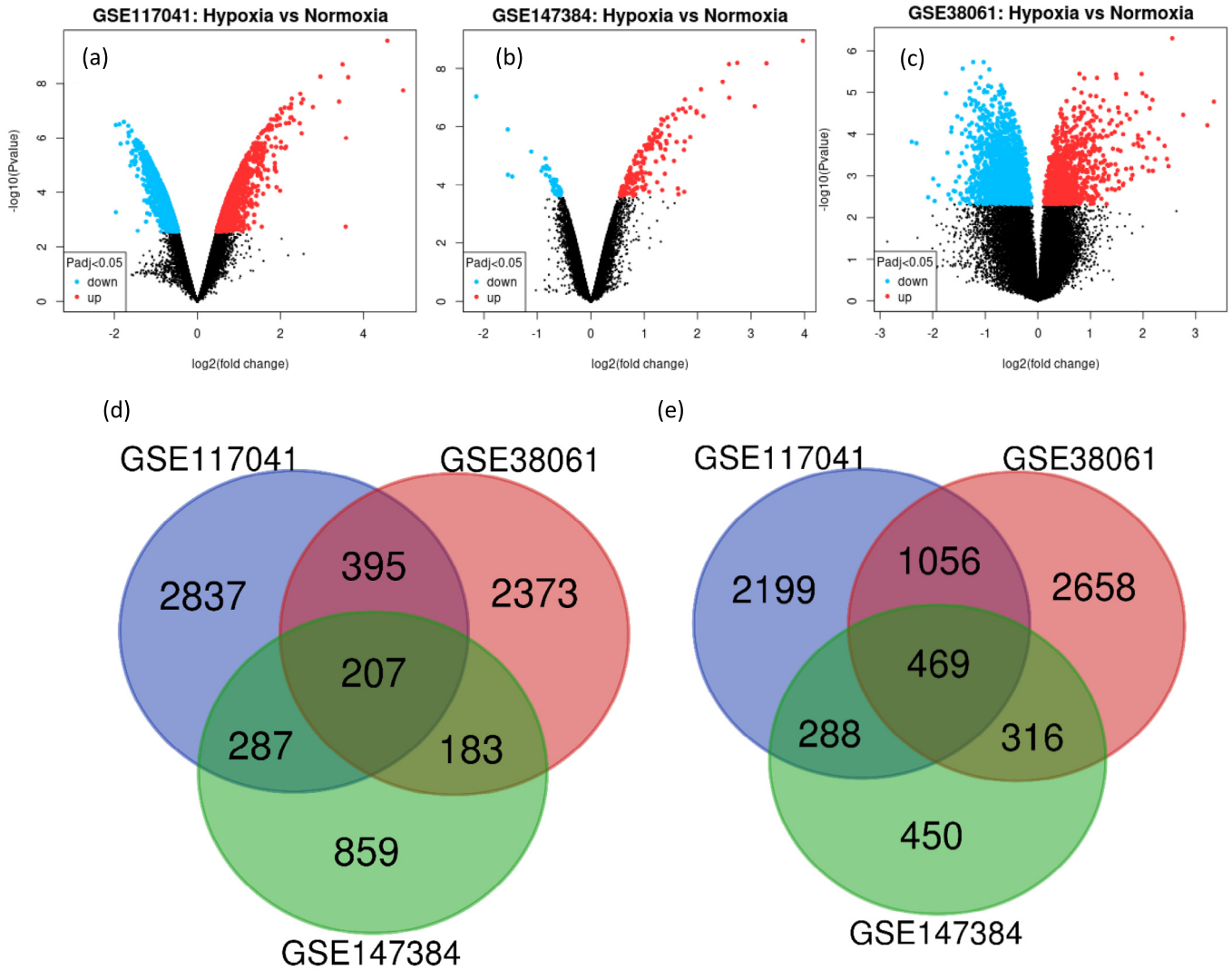

Fig. 1. Evaluation of the overlapping DEGs among GSE11704, GSE147384, and GSE38061 dataSets. (**a**) GSE11704, (**b**) GSE147384, and (**c**) GSE38061, red dots indicate down-regulated while blue dots indicate up-regulated. (**d**) upregulated and (**e**) downregulated cDEGs in hypoxic conditions (log2FC > 0).

Table 1
Gene ontology analysis of DEGs in hypoxic conditions (p value < 0.001).

Expression	Category	Term	Count	%	p-Value	FDR
Upregulated	GOTERM_BP_DIRECT	GO:0001666 ~ response to hypoxia	18	9	2.78E-12	4.27E-09
		GO:0071456 ~ cellular response to hypoxia	15	7.5	1.24E-10	9.50E-08
		GO:0006096 ~ glycolytic process	10	5	3.39E-10	1.74E-07
		GO:0061621 ~ canonical glycolysis	6	3	3.30E-07	1.27E-04
		GO:0043065 ~ positive regulation of apoptotic process	14	7	2.33E-05	0.007159
	GOTERM_CC_DIRECT	GO:0005829 ~ cytosol	89	44.5	4.82E-08	1.33E-05
		GO:0070062 ~ extracellular exosome	46	23	7.94E-07	1.10E-04
		GO:0005737 ~ cytoplasm	80	40	5.34E-05	0.004913
		GO:1904724 ~ tertiary granule lumen	6	3	1.80E-04	0.010699
		GO:1904813 ~ ficolin-1-rich granule lumen	8	4	1.94E-04	0.010699
	GOTERM_MF_DIRET	GO:0051213 ~ dioxygenase activity	6	3	3.82E-05	0.011269
		GO:0031418 ~ L-ascorbic acid binding	5	2.5	5.28E-05	0.011269
		GO:0042802 ~ identical protein binding	35	17.5	1.12E-04	0.015899
		GO:0005515 ~ protein binding	151	75.5	2.19E-04	0.023358
		GO:0005536 ~ glucose binding	4	2	3.40E-04	0.029058
Downregulated	GOTERM_BP_DIRECT	GO:0032543 ~ mitochondrial translation	30	6.651885	2.14E-25	3.60E-22
		GO:0006364 ~ rRNA processing	31	6.873614	2.39E-22	2.01E-19
		GO:0006412 ~ translation	28	6.208426	5.92E-13	3.31E-10
		GO:0006457 ~ protein folding	21	4.656319	1.28E-09	5.38E-07
		GO:1904874 ~ positive regulation of telomerase RNA localization to Cajal body	8	1.773836	1.26E-08	4.25E-06
	GOTERM_CC_DIRECT	GO:0005739 ~ mitochondrion	107	23.72506	9.51E-30	3.82E-27
		GO:0005743 ~ mitochondrial inner membrane	54	11.97339	7.99E-23	1.61E-20
		GO:0005654 ~ nucleoplasm	171	37.91574	2.68E-21	3.59E-19
		GO:0005762 ~ mitochondrial large ribosomal subunit	22	4.878049	6.80E-21	6.83E-19
		GO:0005730 ~ nucleolus	79	17.51663	6.95E-15	5.59E-13
	GOTERM_MF_DIRET	GO:0003723 ~ RNA binding	131	29.04656	5.90E-43	3.81E-40
		GO:0003735 ~ structural constituent of ribosome	30	6.651885	6.56E-16	2.12E-13
		GO:0005515 ~ protein binding	363	80.4878	3.47E-14	7.47E-12
		GO:0034513 ~ box H/ACA snoRNA binding	5	1.108647	1.39E-06	2.25E-04
		GO:0019843 ~ rRNA binding	9	1.995565	3.80E-06	4.90E-04

Table 2
KEGG pathway analysis of DEGs in hypoxic conditions (p value < 0.001).

Expression	Category	Term	Count	%	P value	Genes
Upregulated	KEGG_PATHWAY	hsa04066:HIF-1 signaling pathway	18	9	1.56E-14	EGLN1, MAP2K1, EGLN3, CDKN1B, PFKFB3, SERPINE1, SLC2A1, PRKCA, ENO2, HK2, VEGFA, LDHA, PFKL, PGK1, ALDOC, ALDOA, GAPDH, PFKP
	KEGG_PATHWAY	hsa00010: Glycolysis / Gluconeogenesis	11	5.5	8.54E-09	LDHA, PFKL, TPI1, PGK1, ALDOC, ALDOA, ENO2, GAPDH, PGM1, HK2, PFKP
	KEGG_PATHWAY	hsa00051:Fructose and mannose metabolism	8	4	1.31E-07	PFKFB4, PFKL, PFKFB3, TPI1, ALDOC, ALDOA, HK2, PFKP
	KEGG_PATHWAY	hsa01230: Biosynthesis of amino acids	10	5	3.44E-07	PFKL, TPI1, IDH2, PGK1, ALDOC, ALDOA, ENO2, GAPDH, ASS1, PFKP
	KEGG_PATHWAY	hsa01200:Carbon metabolism	10	5	1.27E-05	PFKL, TPI1, IDH2, PGK1, ALDOC, ALDOA, ENO2, GAPDH, HK2, PFKP
Downregulated	KEGG_PATHWAY	hsa03008: Ribosome biogenesis in eukaryotes	24	5.321508	4.68E-14	POP5, RBM28, POP7, POP1, WDR3, POP4, RPP40, HEATR1, WDR75, IMP4, GTPBP4, GNL3, NOL6, RRP7A, RCL1, EMG1, GNL3L, DKC1, GAR1, NHP2, SBDS, RIOK2, UTP14A, NOP10
	KEGG_PATHWAY	hsa03050: Proteasome	13	2.882483	2.08E-09	PSMD12, PSMD8, PSMA5, PSMB6, PSMB7, PSMD6, PSMA4, PSMB2, PSMB3, PSMC1, PSME3, PSMC2, PSMD1
	KEGG_PATHWAY	hsa03010: Ribosome	22	4.878049	3.47E-09	MRPS17, MRPS15, MRPL18, MRPS12, MRPL19, MRPL36, MRPL15, MRPL12, MRPL13, MRPL24, MRPL21, MRPL32, MRPL22, MRPS18C, MRPL4, MRPL30, MRPL20, MRPL3, MRPS9, MRPL1, MRPL9, RPL26L1
	KEGG_PATHWAY	hsa05014: Amyotrophic lateral sclerosis	26	5.764967	1.68E-05	PSMD12, SEH1L, NUP188, NUP160, PSMD8, PSMB6, PSMB7, PSMD6, PSMB2, PSMB3, CASP3, PSMD1, UQCRFS1, NUP88, UBQLN4, MAP2K3, NDUFA8, SIGMAR1, PSMA5, PSMA4, PSMC1, PSMC2, NDUFS3, SRSF3, NUP35, SRSF7
	KEGG_PATHWAY	hsa03013: Nucleocytoplasmic transport	12	2.660754	1.59E-04	SEH1L, NUP188, TMEM33, CSE1L, NUP35, PHAX, NUP88, RANGAP1, KPNA2, TNPO2, IPO4, NUP160

extracellular exosome, cytoplasm, ficolin-1-rich granule lumen, mitochondrion, mitochondrial inner membrane, tertiary granule lumen, nucleoplasm, mitochondrial large ribosomal subunit, nucleolus, and nucleolus. 3) In the case of molecular function (MF), upregulated DEGs were significantly involved in dioxygenase activity, L-ascorbic acid binding, identical protein binding, protein binding, and glucose binding, whereas downregulated DEGs were enriched in RNA binding, rRNA binding, structural constituent of

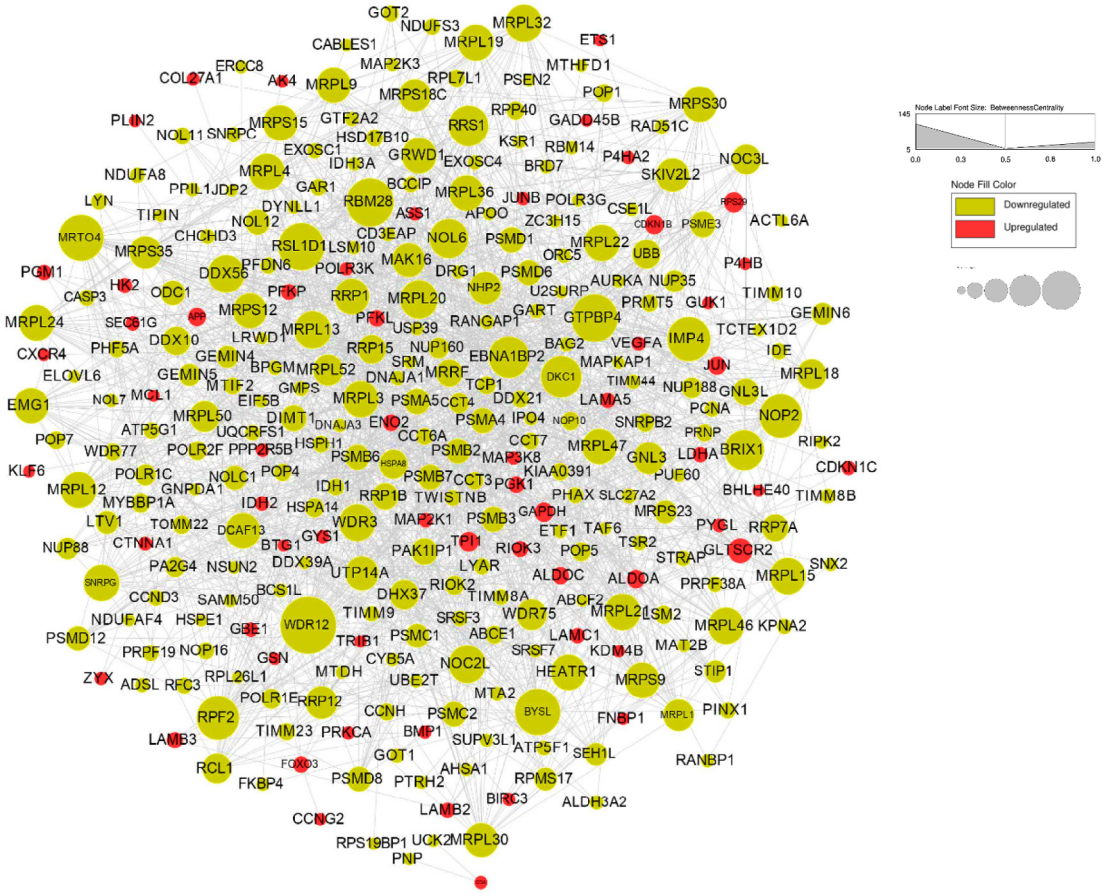

Fig. 2. cDEGs PPI network using the STRING online database and Cytoscape software.

the ribosome, protein binding, box H/ACA snoRNA binding (p-value < 0.001; Table 1).

The outcomes of KEGG analysis revealed that upregulated cDEGs were particularly enriched in the HIF-1 signaling pathway, gluconeogenesis/ glycolysis, biosynthesis of amino acids, carbon metabolism, fructose, and mannose metabolism. In contrast, downregulated cDEGs were enriched in ribosome biogenesis in eukaryotes, proteasome, ribosome, amyotrophic lateral sclerosis, nucleocytoplasmic transport, and spliceosome (P < 0.001; Table 2).

3.3. Building PPI networks, module analysis, and identifying hub genes

To build the PPI network, 676 cDEGs were uploaded to the STRING database (K-means clustering: number of clusters 3, interaction score: highest confidence 0.900). The PPI network is depicted in Fig. 2, with 673 nodes and 1446 edges (PPI enrichment P < 1.0E-16). While a total of 368 GO terms, 20 KEGG pathways, and 147 Reactome pathways were reported in the functional enrichment analysis of the PPI network.

The Cytoscape plugin MCODE was used to identify the most significant modules, with an MCODE score >5 and nodes ≥10. Four significant modules were identified and analyzed using gene ontology. Module 1 was enriched in GO terms like mitochondrial translation, DNA damage response, structural constituent of the ribosome, and RNA binding (Tables S2, S3). Module 2 was enriched in GO terms like regulation of proteasomal protein catabolic process, endopeptidase activity, and enzyme regulator activity. Modules 3 and 4 were involved in RNA processing and ribosome biogenesis (Tables S4, S5). Hub genes were extracted using

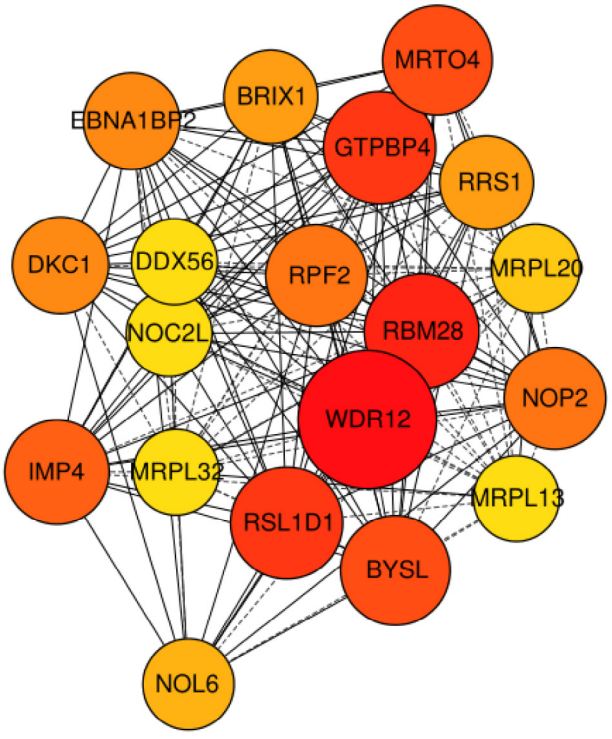

Fig. 3. Screening of Hub genes through Cytoscape's CytoHuba plugin.

Cytoscape software plugin CytoHubba on the PPI network data. The top 19 hub genes were selected as the Hub genes on the basis of the degree algorithm (Fig. 3).

3.4. Hub genes analysis

DAVID tool was used for enrichment analysis of biological processes, cell components, molecular functions, and the KEGG pathway of the 19 hub genes. The findings indicate that all the hub genes except RNA binding motif protein 28 (RBM28) were involved in biological processes i.e., rRNA processing, ribosomal large subunit assembly and biogenesis, translation, etc (Fig. 4a), in the cell components, all the hub genes were involved many components i.e., nucleolus, nucleoplasm, chromosome, etc (Fig. 4b) and in the molecular functions all the hub genes were involved in RNA binding, protein binding, rRNA binding, etc (Fig. 4c). Regarding statistics pathway enrichment of hub genes, they were found to be abundant in 25 pathways from biological processes, cell components, and molecular functions (p-value < 0.05; Fig. 4d). Next, we performed functional annotation clustering using DAVID to cluster the hub genes into common GO functions. Fig. S1 shows the common functions performed by MRPL13, MRPL32, MRPL20, and NOL6 gene clusters. MRPL13, MRPL32, and MRPL20 genes were involved in mitochondria, mitochondrial ribosome, mitochondrial translation, translation, and mitochondrial inner membrane. In contrast, the NOL6 gene was involved in only mitochondria.

In KEGG pathway analysis, five genes (RBM28, DKC1, IMP4, GTPBP4, NOL6) were markedly enriched in ribosome biosynthesis in eukaryotes, and three genes enriched in the ribosome were MRPL20, MRPL13, and MRPL32 (P < 0.05, Table S6; Fig. 5, Fig. 6).

3.5. Hub gene expression and prognostic significance

The significance of 19 hub genes was further validated to identify the survival and expression analyses by GEPIA2 and GTEx studies. GEPIA2 analysis showed that 11 (DKC1, BRIX1, BYSL, EBNAIBP2, GTPBP4, MRPL13, MRTO4, RPF2, RRS1, RSL1D1, and WDR12) out of 19 hub genes were significantly more expressive in one or more of CESC, COAD, and LUAD as shown in Figure S2 and S3 (P < 0.05) as compared to the control cells.

The association between each gene's expression and the average survival time of cancer patients was examined in the hub genes survival analysis. According to the Kaplan-Meier analysis, high expression of DDX56 and IMP4 in LUAD, RBM28 in CESC, and MRPL20 in COAD found (p < 0.05; Fig. S4a). In contrast, high expression of BYSL, MRPL13, MRPL32, RBM28, RPF2, and WDR12 in LAUD and high expression of GTPBP4 and RSL1D1 in CESC had significantly worse survival probability (p < 0.05; Fig. S4b). However, the survival analysis of the remaining 7 hub genes did not reveal a statistically significant association (p > 0.05 and pHR > 0.05).

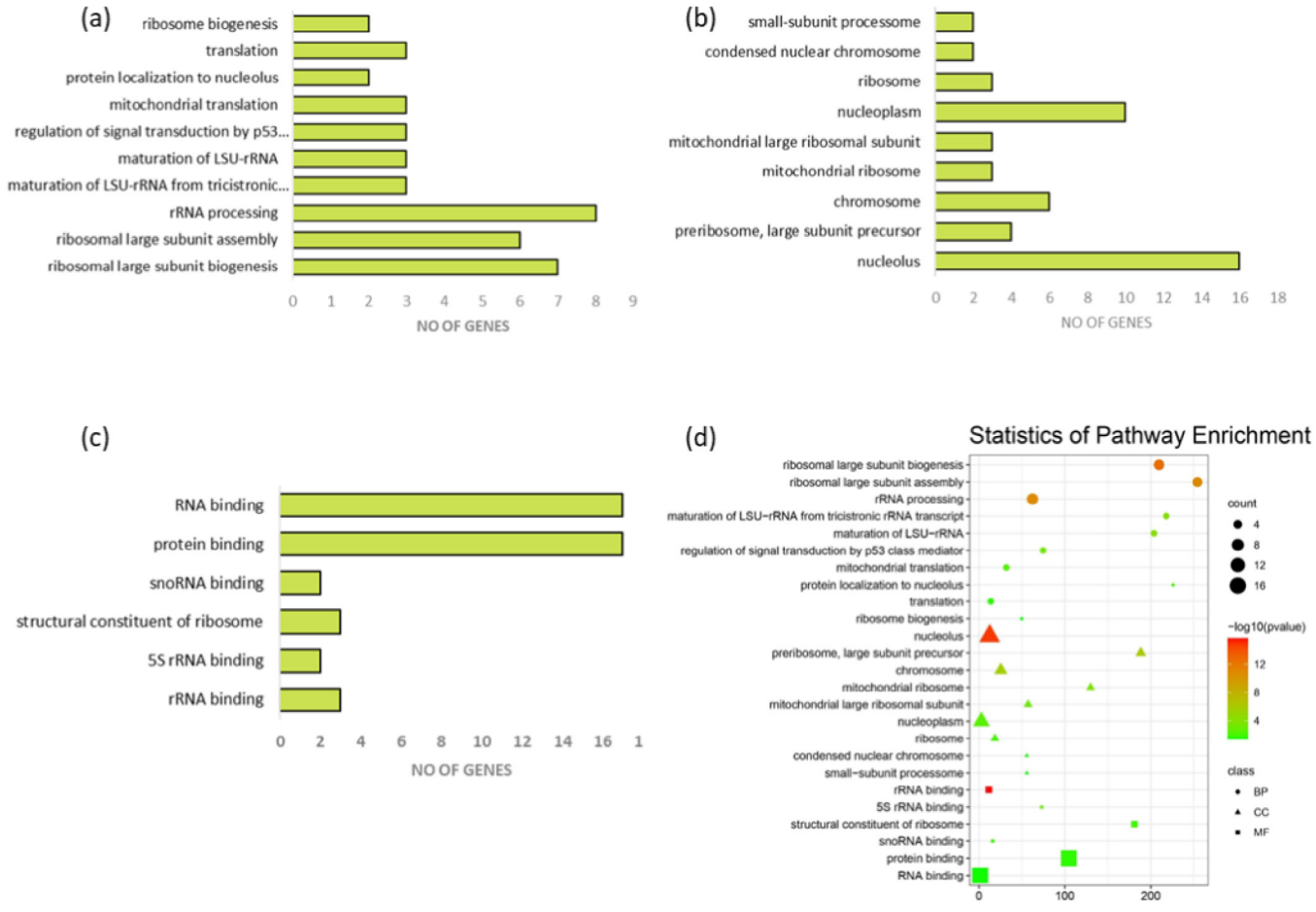

Fig. 4. Gene ontology analysis of hub genes. **(a)** Biological processes, **(b)** Cellular components, **(c)** Molecular functions, and **(d)** Statistics of pathway enrichment of the hub genes.

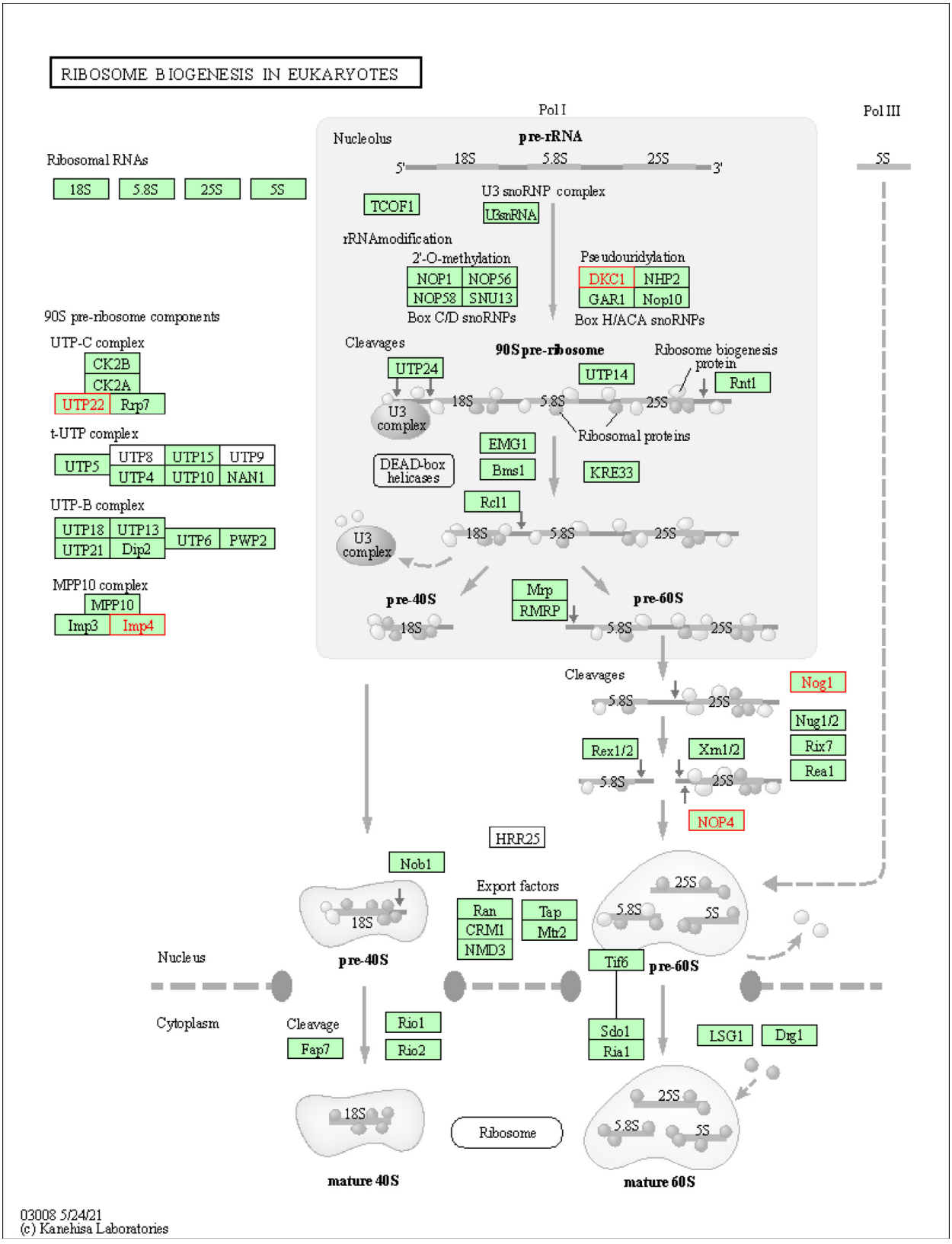

Fig. 5. Ribosome biogenesis pathway; Five genes (RBM28, DKC1, IMP4, GTPBP4, NOL6) were enriched in ribosome biogenesis pathway ($P < 0.05$).

The tissue-specific hub genes' expression in various cancer types is depicted as an interactive heat map in Fig. S5. The target gene expression in various tumor samples was analyzed using a heat map. When compared to other genes, RSL1D1 and MRPL20 were discovered to be significantly expressed in all tumor tissues and may provide more accurate prognostic indicators (Fig. S5).

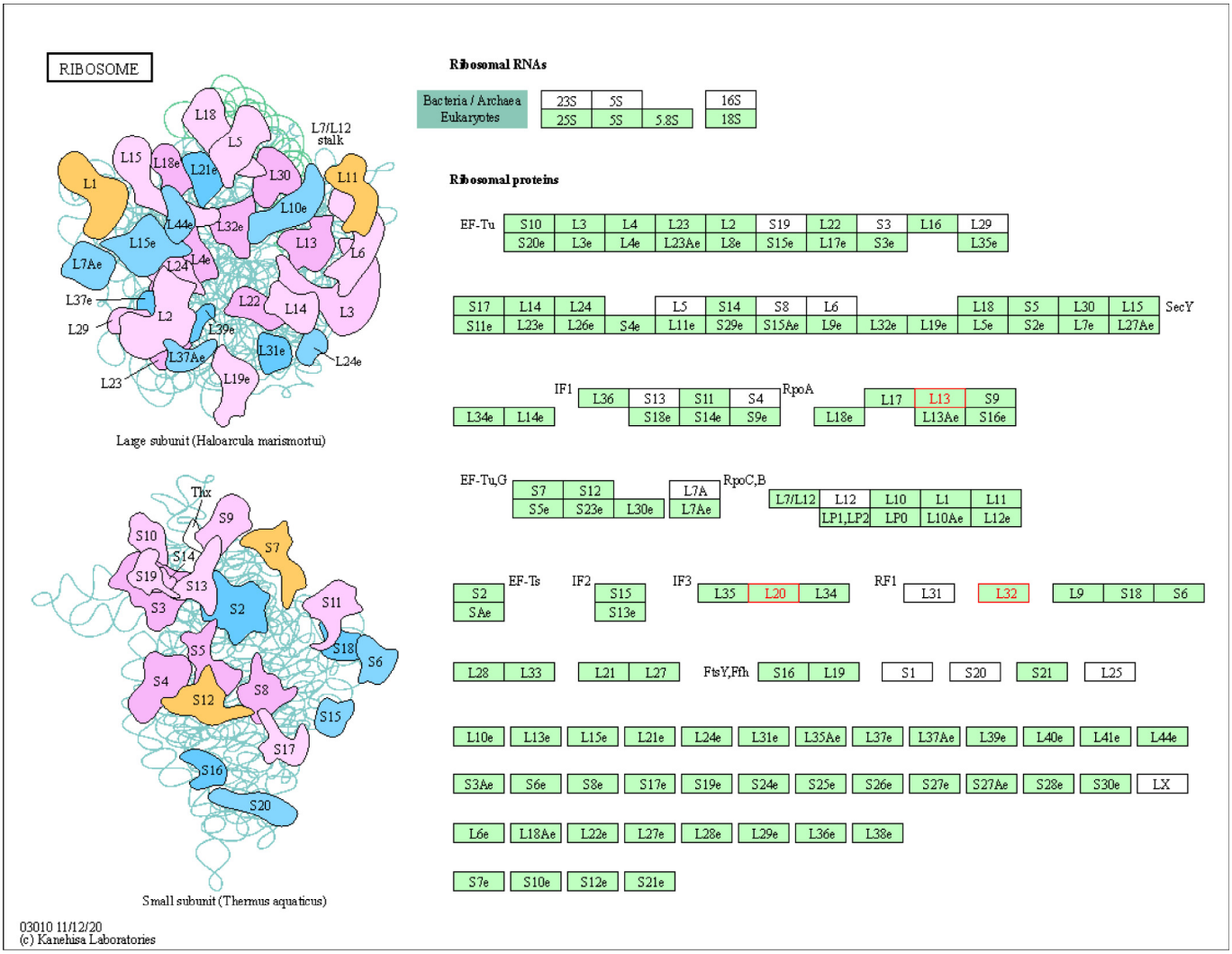

Fig. 6. The ribosome pathway; Three genes (MRPL20, MRPL13, MRPL32) were enriched in ribosome pathway ($P < 0.05$).

4. Discussion

Alteration of metabolic pathways due to hypoxia can enable cells to adapt to the local microenvironment and promote their survival (Sohrabi et al., 2020). Moreover, hypoxia can control the activity of tyrosine kinases receptor and incite a number of signaling pathways that encourage the survival, proliferating, metastasizing, and epithelial-mesenchymal transition (EMT) of tumor cells (Yotnda et al., 2010; Torrisi et al., 2020). Oxygen concentration has been observed to affect chemotherapeutic agents' sensitivity; thus, characterizing and identifying hypoxia-regulated genes in cancer could be advantageous from a therapeutic perspective (Jing et al., 2019).

The current study aimed to examine how hypoxia affects different cancer types. This study analyzed gene expression datasets of lung, colon, and cervical cancer cell lines (A549, HCT116, and HeLa, respectively) under hypoxic and control conditions to identify DEGs using GEO2R online tool (GSE11704, GSE147384, and GSE38061 datasets). A number of 8854 DEGs were verified in GSE11704, 3501 in GSE147384, and 41,379 in GSE38061, with 676 genes differentially expressed in all three datasets. Gene Ontology (GO) and KEGG pathway enrichment analysis of DEGs showed significant enrichment in hypoxic conditions for response to hypoxia, glycolysis, HIF-1 signaling pathway, and ribosome biogenesis. GO analysis and the KEGG pathway confirmed 19 hub genes enrichment in ribosomal biogenesis which were further validated for their expression and prognostic value using GEPIA2 and Kaplan-Meier plotter. Many of our hub genes were significantly upregulated in various cancer cells compared to the normal cells when analyzed by GEPIA2. However, some of the hub genes were not significantly upregulated. Interestingly, these genes cause high survival probability when highly expressed in any cancer type (DDX56 and IMP4 in LUAD, RBM28 in CESC, and MRPL20 in COAD), as shown by Kaplan-Meier plots. These four genes can perform the tumor suppressor function in respective cancer types and can be effectively targeted (Lu et al., 2021).

In contrast to the above findings, all of the hub genes, found in our study were downregulated in hypoxic conditions than in normoxia as shown by Geo2R data. Then, why GEPIA2 analysis gives us their high expression in cancer cells? One of the possible answers to this question is that cancer cells respond differently in hypoxic conditions, as proved by many studies (Nakayama and Kataoka, 2019; Ke et al., 2019). It is not inappropriate to say that the outer cells of the tumor mass respond differently to the tumor microenvironment than the inner cells. This results in heterogeneity in gene expression of the different tumor cells (Nakayama and Kataoka, 2019).

One of the most important findings of this study is that all of our hub genes belong to ribosome biogenesis, as confirmed by GO and KEGG pathway analysis. It is a well-studied phenomenon that ribosomal biogenesis alters in cancer cells. The nucleolar organizer regions (NORs) of the genome, organized in repetitive patterns, are typically engaged in ribosomal biogenesis (McStay, 2016). The resulting 47S pre-rRNA transcript is a single polycistronic molecule that undergoes further modifications within the nucleolus. Co-transcriptional initiation and a number of processing steps, such as endo- and exonucleolytic cleavages, pseudouridylation, and 2′-O-methylation, are all a part of the maturation process (Henras et al., 2015). The small ribosomal subunit (SSU) contains the 18S rRNA, whereas the large ribosomal subunit (LRS) contains the 5.8S, 28S, and 5S rRNA (LSU) (Turi et al., 2019) but in cancer cells, 2′-O-methylation patterns vary as compared to normal cells (Marcel et al., 2015). In these cells, alterations in 2′-O-methylation have been reported, with some studies showing an overall decrease in the levels of 2′-O-methylation (Turi et al., 2019). These changes in 2′-O-methylation have been associated with alterations in the expression of RNA methyltransferases and changes in ribosome composition, which can affect the translational landscape of cancer cells and contribute to their malignant phenotype (Elhamamsy et al., 2022).

Hypoxia can also affect 2′-O-methylation levels in cells but in a different way. Under hypoxic conditions, cells activate various adaptive mechanisms to promote cell survival, including ribosome biogenesis and function changes. Some studies have shown that hypoxia can lead to an increase in the levels of 2′-O-methylation in specific nucleotides of rRNA, which may play a role in promoting cell survival and adaptation to low oxygen conditions (Erales et al., 2017; Metge et al., 2021). Thus, it is clear that the tumor cells respond differently in the presence and absence of oxygen in many aspects, one of which is ribosome biogenesis. This ribosomal biogenesis in cancer cells with and without hypoxia could be a better target for treating hypoxic tumors (bigger tumors). We identified 11 significant genes which expressed differently in tumors with and without hypoxia. These genes could prove better prognosis markers to identify cancers with and without a hypoxic microenvironment.

5. Conclusion

Our bioinformatics analysis revealed that 11 genes (DKC1, BRIX1, BYSL, EBNAIBP2, GTPBP4, MRPL13, MRTO4, RPF2, RRS1, RSL1D1, and WDR12) were downregulated in hypoxic tissues compared to normoxic tissues. These genes were identified as promising prognostic markers and were found to play crucial roles in the development and progression of hypoxic tumors. Additionally, we identified four genes (DDX56 and IMP4 in LUAD, RBM28 in CESC, and MRPL20 in COAD) as potential tumor suppressors. However, further research is necessary to verify our predictions and comprehend the underlying mechanisms. Such findings offer new perspectives and insights into exploring molecular markers and potential therapeutic targets for cancer.

6. Funding

No funding was received for this work from any organization.

7. Authors' contributions

FA collected and wrote the manuscript. NS helped in data analysis. AR helped in manuscript editing.

Declaration of Competing Interest

The authors declare that they have no known competing financial interests or personal relationships that could have appeared to influence the work reported in this paper.

Appendix A. Supplementary material

Supplementary data to this article can be found online at https://doi.org/10.1016/j.sjbs.2023.103752.

References

Bartoszewski, R., Moszyńska, A., Serocki, M., Cabaj, A., Polten, A., Ochocka, R., Dell'Italia, L., Bartoszewska, S., Króliczewski, J., Dąbrowski, M., Collawn, J.F., 2019. Primary endothelial cell–specific regulation of hypoxia-inducible factor (HIF)-1 and HIF-2 and their target gene expression profiles during hypoxia. FASEB J. 33 (7), 7929–7941.
Baxevanis, A.D., Bader, G.D., Wishart, D.S., 2020. Bioinformatics. John Wiley & Sons.
Dekker, Y., Le Dévédec, S.E., Danen, E.H., Liu, Q., 2022. Crosstalk between hypoxia and extracellular matrix in the tumor microenvironment in breast cancer. Genes 13 (9), 1585.
Elhamamsy, A.R., Metge, B.J., Alsheikh, H.A., Shevde, L.A., Samant, R.S., 2022. Ribosome biogenesis: a central player in cancer metastasis and therapeutic resistance. Cancer Res. 82 (13), 2344–2353.
Erales, J., Marchand, V., Panthu, B., Gillot, S., Belin, S., Ghayad, S.E., et al., 2017. Evidence for rRNA 2′-O-methylation plasticity: control of intrinsic translational capabilities of human ribosomes. Proc. Nat. Acad. Sci. 114 (49), 12934–12939.
Fares, C.M., Van Allen, E.M., Drake, C.G., Allison, J.P., Hu-Lieskovan, S., 2019. Mechanisms of resistance to immune checkpoint blockade: why does checkpoint inhibitor immunotherapy not work for all patients? Am. Soc. Clin. Oncol. Educ. Book 39, 147–164.
Ferrari, A., Stark, D., Peccatori, F.A., Fern, L., Laurence, V., Gaspar, N., Bozovic-Spasojevic, I., Smith, O., De Munter, J., Derwich, K., Hjorth, L., van der Graaf, W.T. A., Soanes, L., Jezdic, S., Blondeel, A., Bielack, S., Douillard, J.-Y., Mountzios, G., Saloustros, E., 2021. Adolescents and young adults (AYA) with cancer: a position paper from the AYA working group of the European Society for Medical Oncology (ESMO) and the European Society for Paediatric Oncology (SIOPE). ESMO Open 6 (2), 100096.
Fojtík, P., Beckerová, D., Holomková, K., Šenfluk, M., Rotrekl, V., 2021. Both hypoxia-inducible factor 1 and MAPK signaling pathway attenuate PI3K/AKT via suppression of reactive oxygen species in human pluripotent stem cells. Front. Cell Develop. Biol. 8, 607444.
Henras, A.K., Plisson-Chastang, C., O'Donohue, M.F., Chakraborty, A., Gleizes, P.E., 2015. An overview of pre-ribosomal RNA processing in eukaryotes. Wiley Interdisc. Rev. RNA 6 (2), 225–242.
Hiatt, R.A., Beyeler, N., 2020. Cancer and climate change. Lancet Oncol. 21 (11), e519–e527.
Hu-Lieskovan, S., Malouf, G.G., Jacobs, I., Chou, J., Liu, L., Johnson, M.L., 2021. Addressing resistance to immune checkpoint inhibitor therapy: an urgent unmet need. Fut. Oncol. 17 (11), 1–39.
Jiang, F., Miao, X.-L., Zhang, X.-T., Yan, F., Mao, Y., Wu, C.-Y., Zhou, G.-P., Ji, J., 2021. A hypoxia gene-based signature to predict the survival and affect the tumor immune microenvironment of osteosarcoma in children. J. Immunol. Res. 2021, 1–13.
Jing, X., Yang, F., Shao, C., Wei, K., Xie, M., Shen, H., Shu, Y., 2019. Role of hypoxia in cancer therapy by regulating the tumor microenvironment. Mol. Cancer 18, 1–15. 5523832.
Ke, X., Chen, C., Song, Y., Cai, Q., Li, J., Tang, Y., et al., 2019. Hypoxia modifies the polarization of macrophages and their inflammatory microenvironment, and inhibits malignant behavior in cancer cells. Oncol. Lett. 18 (6), 5871–5878.
Lee, P., Chandel, N.S., Simon, M.C., 2020. Cellular adaptation to hypoxia through hypoxia inducible factors and beyond. Nat. Rev. Mol. Cell Biol. 21 (5), 268–283.
Leng, A., Jing, J., Nicholas, S., Wang, J., 2019. Catastrophic health expenditure of cancer patients at the end-of-life: a retrospective observational study in China. BMC Palliat Care 18, 1–10.
Lu, M., Fan, X., Liao, W., Li, Y., Ma, L., Yuan, M., et al., 2021. Identification of significant genes as prognostic markers and potential tumor suppressors in lung adenocarcinoma via bioinformatical analysis. BMC Cancer 21 (1), 1–13.
Marcel, V., Catez, F., Diaz, J.-J., 2015. Ribosome heterogeneity in tumorigenesis: the rRNA point of view. Mol. Cell Oncol. 2 (3), e983755.
McStay, B., 2016. Nucleolar organizer regions: genomic 'dark matter requiring illumination. Genes Dev. 30 (14), 1598–1610.
Metge, B.J., Kammerud, S.C., Pruitt, H.C., Shevde, L.A., Samant, R.S., 2021. Hypoxia reprograms 2'-O-Me modifications on ribosomal RNA. iScience 24 (1), 102010.
Muz, B., de la Puente, P., Azab, F., Azab, A.K., 2015. The role of hypoxia in cancer progression, angiogenesis, metastasis, and resistance to therapy. Hypoxia 3, 83–92.
Nakayama, K., Kataoka, N., 2019. Regulation of gene expression under hypoxic conditions. Int. J. Mol. Sci. 20 (13), 3278.

Ponomarev, A., Gilazieva, Z., Solovyeva, V., Allegrucci, C., Rizvanov, A., 2022. Intrinsic and extrinsic factors impacting cancer stemness and tumor progression. Cancers 14 (4), 970.
Rosenbaum, M.W., Gonzalez, R.S., 2021. Targeted therapy for upper gastrointestinal tract cancer: current and future prospects. Histopathology 78 (1), 148–161.
Sohrabi, E., Behranvand, N., Moslemi, M., Namdar, A., Khani, P., 2020. Identification of key genes in breast cancer cell line under hypoxia condition: a bioinformatics analysis. Int. J. Biomed. Public Health 3 (3), 62–69.
Tan, Y., Luo, X., Lv, W., Hu, W., Zhao, C., Xiong, M., et al., 2021. Tumor-derived exosomal components: the multifaceted roles and mechanisms in breast cancer metastasis. Cell Death Disease 12 (6), 547.
Torrisi, F., Vicario, N., Spitale, F.M., Cammarata, F.P., Minafra, L., Salvatorelli, L., et al., 2020. The role of hypoxia and SRC tyrosine kinase in glioblastoma invasiveness and radioresistance. Cancers 12 (10), 2860.
Turi, Z., Lacey, M., Mistrik, M., Moudry, P., 2019. Impaired ribosome biogenesis: mechanisms and relevance to cancer and aging. Aging 11 (8), 2512–2540.
Ulldemolins, A., Seras-Franzoso, J., Andrade, F., Rafael, D., Abasolo, I., Gener, P., Schwartz, J.R.S., 2021. Perspectives of nano-carrier drug delivery systems to overcome cancer drug resistance in the clinics. Cancer Drug Resist. 4 (1), 44.
Yotnda, P., Wu, D., Swanson, A.M., 2010. Hypoxic tumors and their effect on immune cells and cancer therapy. Immunother. Cancer: Methods Protocols 2010, 1–29.